ChemComm

Accepted Manuscript

This article can be cited before page numbers have been issued, to do this please use: S. M. Draper, J. Wang, Y. Lu, W. McCarthy, R. Conway-Kenny, B. Twamley and J. Zhao, *Chem. Commun.*, 2017, DOI: 10.1039/C7CC08535D.


Volume 52 | Number 1 | 4 January 2016 | Pages 1–216

ChemComm
Chemical Communications
www.rsc.org/chemcomm

ISSN 1359-7345

ROYAL SOCIETY OF CHEMISTRY

COMMUNICATION

175 YEARS

ROYAL SOCIETY OF CHEMISTRY

rsc.li/chemcomm

View Article Online
DOI: 10.1039/C7CC08535D

Journal Name

COMMUNICATION

Novel ruthenium and iridium complexes of *N*-substituted carbazole as triplet photosensitisers

Received 00th January 20xx,
Accepted 00th January 20xx

DOI: 10.1039/x0xx00000x

www.rsc.org/

Junsi Wang,[a] Yue Lu,[a] William McCarthy,[a] Robert Conway-Kenny,[a] Brendan Twamley,[a] Jianzhang Zhao,[b] and Sylvia M. Draper[a*]

Novel mono- and di-nuclear Ru(II) and Ir(III) complexes, bearing a modified carbazole moiety are synthesised. In comparison to their mononuclear analogues, the homonuclear diatomic complexes (RuCRu and IrCIr), in which the carbazole containing-ligand functions as a bridge, display increased absorbance in the visible region, and give rise to higher singlet oxygen quantum yields.

Triplet photosensitisers are finding increased application in photoredox catalytic reactions,[1] photoinduced H_2 production,[2] photodynamic therapy,[3] triplet-triplet annihilation upconversion,[4-8] photovoltaics,[9] and photoswitching.[10] Most are transition metal complexes, due to their near unity intersystem crossing (ISC) efficiency, but suffer from weak absorbance in the visible region and shortened triplet excited state lifetimes.[11] Ziessel and co-workers have reported a series of dinuclear Ru-terpy derivatives,[12, 13] utilising bridging ligands (which include phenylenic and acetylenic hydrocarbons, and aromatic units such as benzene, naphthalene, anthracene, and pyrene), that appear to overcome some of these short-comings. Their dinuclear complexes, possessing highly conjugated ligands appear to exhibit longer triplet excited state lifetimes, and to out-perform their mononuclear analogues in terms of molar absorptivity.[14,15] Despite their promise, dinuclear complexes of Ru(II) or Ir(III) are rarely used for Triplet-Triplet Annihilation Upconversion (TTA-UC)[16], and only limited data are available for the d^8 Pt(II) based dinuclear complexes encountered in the literature.[17-19] In a recent study,[20] we demonstrated that the introduction of a second transition metal centre can significantly enhance and red-shift the absorbance into the NIR region, and lead to prolonged triplet lifetimes. In this latest work, we develop the dinuclear concept further, using it in the design of triplet photosensitisers for applications in TTA-UC, and singlet oxygen ($^1O_2$) photosensitisation. To this end a new and extended N-substituted carbazole bridging ligand was designed and synthesised to exploit the known electron-rich and electron-donating character of the carbazole moiety and to act as a connector between two photoresponsive metal centres.

Two dinuclear complexes (**RuCRu** and **IrCIr**), and two mononuclear complexes (**RuC** and **IrC**) were generated and their triplet photosensitising capabilities compared. To ensure an extended π-conjugated ligand structure, acetylene moieties were incorporated between the ligating bipyridine units and the N-substituted carbazole. All the compounds were obtained in moderate to good yields. (See ESI for detailed synthetic information and full spectroscopic characterisation of **RuC**, **RuCRu**, **IrC**, **IrCIr** and single crystal diffraction data for **RuC**).

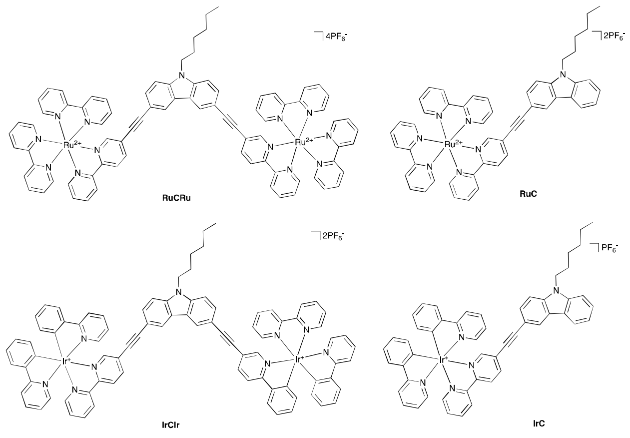

Chart 1. Chemical structures of the novel **RuCRu**, **RuC**, **IrCIr** and **IrC** complexes.

The absorption spectra of the mono- and di-nuclear N-substituted carbazole complexes are shown in Figure 1a. The enhanced molar absorptivities (ε) of the dinuclear structures are immediately apparent e.g. the ε value of **RuCRu** (ε = 62,000 M^{-1} cm^{-1}, λ_{abs} = 412 nm) is approximately twice that of

---

[a] *School of Chemistry, University of Dublin, Trinity College, Dublin 2, Ireland.*
[b] *State Key Laboratory of Fine Chemicals, School of Chemical Engineering, Dalian University of Technology, E208 Western Campus, 2 Ling-Gong Road, Dalian 116012, P. R. China.*

†Electronic Supplementary Information (ESI) available: The single crystal data of **RuC**, **CCDC no. 1566335**. ; the synthesis and characterisation data of the complexes; details of photophysical properties; details of TTA upconversion; details of DFT calculation. See DOI: 10.1039/x0xx00000x

View Article Online
DOI: 10.1039/C7CC08535D

its mononuclear analogue, **RuC** (ε = 25,000 M^{-1} cm^{-1}, λ_{abs} = 411 nm). A similar trend is seen for **IrCIr** and **IrC** (Table 2).

The intense absorptions at around 288 nm were assigned to the $\pi \rightarrow \pi^*$ transition of the parent 2,2'-bipyridine ligands (in Ru complexes) and the bands at ~412 nm (in the Ru complexes) and ~400 nm (in the Ir complexes) were assigned to the $\pi \rightarrow \pi^*$ transition of the ancillary carbazole-substituted bipyridine ligand.[21] The low-energy shoulder at approximately 470 nm in the spectra of **RuCRu** and **RuC** is predominately attributed to a metal to ligand charge transfer (^{1}MLCT). In both cases it is bathochromically shifted by 20 nm compared to that of $[Ru(bpy)_3]^{2+}$.[22] This red-shift is a consequence of the enlarged π-conjugated carbazole, which serves to decrease the energy of the ligand-centred lowest unoccupied molecular orbital (LUMO) and thereby reduce the HOMO-LUMO gap in these complexes.

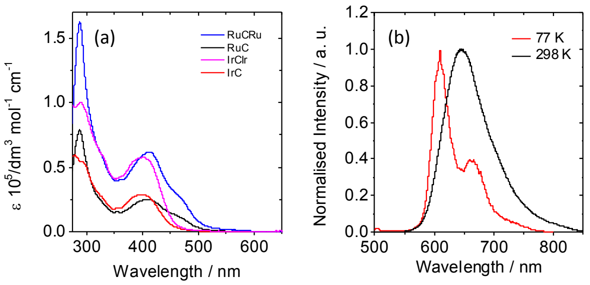

Figure 1. a) UV-Vis absorption spectra of **RuCRu**, **RuC**, **IrCIr** and **IrC**. C = 1.0 × 10^{-5} M in CH_3CN, 298 K. b) The normalised emission spectra of **RuCRu** at low temperature (77 K), and at room temperature (298 K). C = 1.0 × 10^{-5} M in CH_3CH_2OH/CH_3OH (4:1, v/v).

To support these assignments, the electrochemical properties of the complexes were studied *via* cyclic voltammetry measurements (Table 1 and Figure S14). Each metal complex shows only one oxidation. In the case of **RuC** and **RuCRu** the oxidation potentials are very similar to each other and to the Ru(II/III) redox couple of $[Ru(bpy)_3]^{2+}$[23]. The oxidations determined for the bimetallic complexes are believed to be one-electron processes. They involve just one metal centre, with the oxidation of the second metal occurring outside the acetonitrile solvent window and at a considerably higher potential (consistent with the work of Salpage *et al.*[24]). The *quasi*-reversible (ΔE_p value > 60 mV) oxidation wave for **RuCRu** is indicative of contributions from the ligand to the HOMO. For each of **RuC**, **IrC** and **IrCIr** the oxidation process is clearly irreversible further suggesting significant ligand-character in the HOMOs. Additional support for this assertion is provided by TD-DFT based on the ground-state optimised geometries (Table S1-4).

There are two ligand-centred reductions observed for the ruthenium complexes. The first reduction potential in both **RuCRu** and **RuC** is higher (less negative) than those reported for $[Ru(bpy)_3]^{2+}$ (Table 1). This suggests that the LUMOs are being stabilised by the delocalised and highly conjugated nature of the carbazole extension (as supported by TD-DFT analyses, Table S1-4). The second reduction occurs more readily in **RuCRu** than **RuC** because of the electron withdrawing effect of two metal centres. The sharp redox waves seen in the cyclic voltammograms of **RuCRu** and **IrCIr** (Figure S14) are consistent with electroprecipitation occurring at these potentials.[25, 26]

Table 1. Electrochemical Potentials vs. Fc(+/0) [a]

Compound	Oxidation(V)[ΔE_P(mV)]	Reduction(V) [ΔE_P(mV)]
RuCRu	+0.93[94]	–1.58[62]; –1.82[92][d1]
RuC	+0.94[--][c]	–1.58[55]; –1.88[76]
IrCIr	+0.99[--][c]	–1.56[88][d2]
IrC	+0.95[--][c]	–1.59[56]
$[Ru(bpy)_3]^{2+}$ [b]	+0.90	-1.77; -1.97; -2.21
$[Ir(ppy)_2(bpy)]^+$ [26]	--	-1.83

[a] Cyclic voltammetry in deaerated CH_3CN containing a 0.10 M Bu_4NPF_6 supporting electrolyte; the counter electrode is a Pt electrode; the working electrode is a glassy carbon electrode; the $Ag/AgNO_3$ couple is the reference electrode. Ferrocene (Fc) was used as an internal reference. C[Ag^+] = 0.1 M; 0.5 mM photosensitiser in deaerated CH_3CN at 298 K. [b] These values were calculated from a literature source.[23] [c] Irreversible process, E_{pa} [d] Electroprecipitation effect on reduction. [d1] E_{pc} = –1.86 V; E_{pa} = –1.77 V. [d2] E_{pc} = –1.60 V; E_{pa} = –1.52 V.

The emission properties of the generated complexes were studied in air and under nitrogen. For **RuCRu**, the intense emission at 644 nm is quenched in an aerated solution, and has a microsecond scale lifetime (1.2 μs), consistent with a strong phosphorescence character (Figure S12a). Compared to $[Ru(bpy)_3]^{2+}$,[22] the phosphorescence emission is bathochromically shifted (by 37 nm), and the excited state lifetime is also prolonged (from 0.8 μs to 1.2 μs). Similar results were found for **RuC**, **IrCIr** and **IrC** (Figure S15, and compared with $\tau_p[Ir(ppy)_2(bpy)]^+$ = 0.3 μs[28]).

Both the mononuclear and dinuclear complexes showed a large thermal anti-Stokes shift at 77 K (Figure 1b and Figure S13). This anti-Stokes shift (900–1900 cm^{-1}) indicates the presence of charge transfer (CT) processes.[1] The profile of the emission bands arising from triplet metal-to-ligand charge transfer (^{3}MLCT) states are generally broad and featureless, compared to those of ligand-based ($^3\pi-\pi^*$) states that are more likely to be highly structured at room temperature. Therefore, we can assign considerable ^{3}MLCT character to the emission.

Table 2. Photophysical data of the generated complexes. [a]

	λ_{abs} (nm)	ε [b]	λ_{em} [c] (nm)	Φ_P [d](%)	τ_P [e](μs)
RuCRu	288; 412	1.63; 0.62	644	6.7	1.2 [e1]/4.7 [e2]
RuC	288; 411	0.79; 0.25	642	6.9	1.3 [e1]/3.9 [e2]
IrCIr	288; 400	1.00; 0.58	614	5.0	0.4 [e1]/2.7 [e2]
IrC	279; 399	0.59; 0.29	613	8.3	0.9 [e1]/5.0 [e2]

[a] Results of complexes in CH_3CN solution (1 × 10^{-5} M), 298 K. [b] Molar absorption coefficient, ε 10^5 dm^3 mol^{-1} cm^{-1}. [c] Emission peak at 298 K in N^2. [d] Quantum yield of phosphorescence, in N_2, with 2,6-diiodo-BODIPY as a standard (Φ_f = 2.7% in CH_3CN).[29] [e] Phosphorescence lifetime, λ_{ex} = 403 nm, at 298 K ([e1]) and 77 K ([e2]) in N_2.

To further explore the nature of the triplet excited states, nanosecond time-resolved transient absorption difference spectra were obtained. Upon excitation, a significant bleaching peak at 400 nm was observed *e.g.* in **RuCRu** (Figure 2a). This corresponds to intraligand charge transfer (ILCT) transitions

View Article Online
DOI: 10.1039/C7CC08535D

within the ancillary carbazole-substituted bipyridine ligand, indicating that the triplet excited state of **RuCRu** is at least partially localised here. Clearly, the triplet excited states of **RuCRu** contain both ^{3}ILCT and ^{3}MLCT character. Comparison with the transient absorption spectrum of $[Ru(bpy)_3]^{2+}$ (Figure 2b), indicates that the ^{3}MLCT bleaching peak of **RuCRu** (expected at approx. 450 nm) would overlap with the strong positive signal at 425–750 nm from the ancillary carbazole-substituted bipyridine ligand. These results were not unique to **RuCRu**, but are similar to those also obtained for **RuC**, **IrClr** and **IrC** (Figure S15). The triplet lifetimes of the complexes are presented in Table 3.

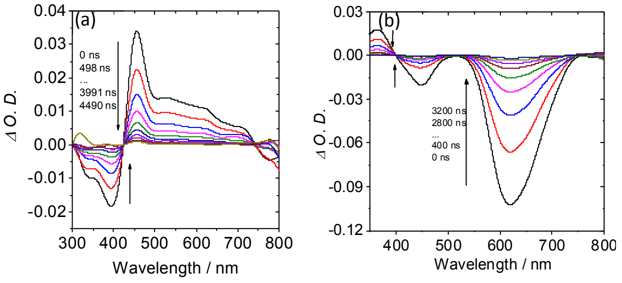

Figure 2. The nanosecond time-resolved transient difference absorption spectra of a) **RuCRu** and b) $\mathbf{[Ru(bpy)_3]^{2+}}$. C = 1.0 × 10^{-5} M in deaerated CH_3CN, 298 K.

In order to confirm the overlapping nature of the ^{3}ILCT and ^{3}MLCT of **RuCRu**, density functional theory (DFT) calculations were carried out. The isosurface spin density of the triplet states were computed using the optimised geometry of the complex. Shown in Figure 3, the triplet spin density is located on both the large ancillary carbazole-substituted bipyridine ligand, and the coordinated metal centre. (See time-dependent DFT calculation results of all generated complexes in ESI, section 8.0)

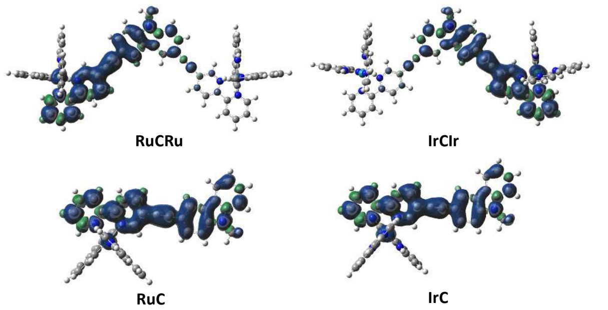

Figure 3. Isosurfaces of spin density of **RuCRu**, **RuC**, **IrClr** and **IrC** at the optimised triplet-state geometries. CH_3CN was used as the solvent in the calculations. Calculations were performed at TDDFT/B3LYP/GENECP/LANL2DZ level with Gaussian 09.

Each complex was studied as a photosensitiser in triplet-triplet annihilation upconversion (TTA-UC). In a standard TTA-UC process, the triplet photosensitiser is excited by an external light source (approximate power density output of 70.8 mW·cm^{-2}). Energy transfer occurs from the photosensitiser to the acceptor molecule *via* intermolecular triplet–triplet energy transfer (TTET). The singlet excited state of the acceptor is accessed *via* TTA between the collision of two triplet excited state acceptors, generating upconverted fluorescence. 9,10-diphenylanthracene (DPA) was used as the optimal triplet acceptor according to the absorption and triplet excited state energy levels of the photosensitisers.

Upon excitation at 473 nm in deaerated solution, **RuCRu** phosphoresces at 644 nm (Figure 4a). Upon the addition of DPA, the phosphorescence decreases significantly, and a new luminance at 430 nm appears. This new emission band is the upconverted fluorescence of DPA, which cannot be achieved by excitation at 473 nm alone. The upconversion quantum yield for **RuCRu** was determined as 21.6%. For **IrClr**, in the presence of DPA, the upconversion quantum yield was calculated as 15.3%. The upconversion quantum yields of their mononuclear analogues were also determined (Φ_{UC} = 19.1% for **RuC**, and Φ_{UC} = 19.0% for **IrC**) (Figure S16). There is no significant improvement between the data obtained for the dinuclear and mononuclear complexes.

The TTET efficiencies of the generated complexes were determined by triplet state lifetime quenching studies (in the presence of the triplet acceptor, DPA). The resulting Stern-Volmer quenching curves were then plotted (Figure 4b). The quenching of the triplet state of **IrClr** was found to be the least efficient, and this may be due to its short-lived triplet excited state lifetime. A comparison of the data obtained is provided in Table 3. Time-resolved emission spectra were also collected (Figure 4c).

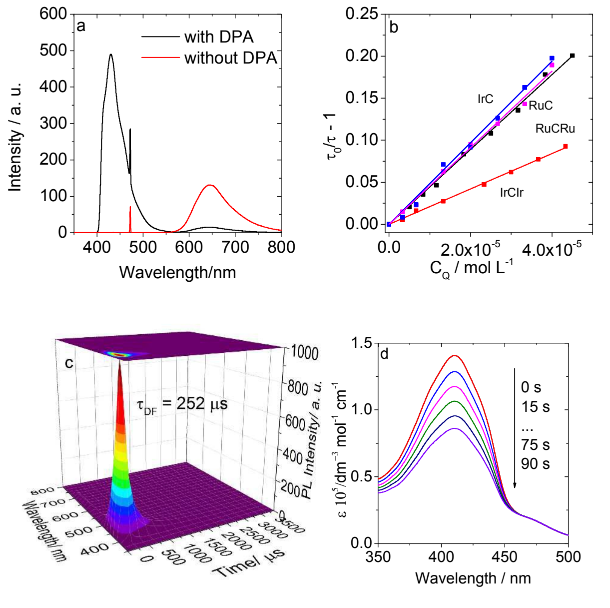

Figure 4. a) Upconversion with **RuCRu** as the triplet photosensitiser, and DPA as the triplet acceptor. C[**RuCRu**] = 1.0 × 10^{-5} M and C[DPA] = 2.0 × 10^{-3} M in deaerated CH_3CN, 298 K. b) The Stern-Volmer plots generated from the triplet excited state lifetime quenching as a function of DPA concentration in deaerated CH_3CN at 298 K. C[photosensitiser] = 1.0 × 10^{-5} M. c) Time-resolved emission spectrum of **RuCRu** and the upconverted fluorescence of DPA using **RuCRu** as triplet photosensitiser on excitation with nanosecond OPO laser. C[**RuCRu**] = 1.0 × 10^{-5} M and C[DPA] = 2.0 × 10^{-3} M in deaerated CH_3CN, 298 K. d) $^1O_2$ photosensitisation: Irradiation time-dependent decrease of absorption at 410 nm of DPBF with **RuCRu** as the photosensitiser. λ_{ex} = 436 nm in CH_3CN at 298 K.

View Article Online
DOI: 10.1039/C7CC08535D

The upconverted fluorescence lifetime of **IrCIr** at 386 μs, was much longer than that of the other three complexes (Figure S17). This is likely related to its short triplet excited lifetime, and consequently less efficient TTET.

Table 3. Triplet state properties of the generated complexes. [a]

	τ_T [b](μs)	τ_{DF} [c](μs)	K_{SV} [d](M^{-1})	k_q [e]($10^6\ M^{-1}\ s^{-1}$)	Φ_{UC} [f](%)	Φ_Δ [g](%)
RuCRu	1.2	252	4448	3706	21.6	83.3
RuC	1.2	284	4477	3197	19.1	56.3
IrCIr	0.4	386	2102	5255	15.3	67.2
IrC	0.9	301	4809	5343	19.0	54.1

[a] Results of complexes in CH_3CN solution (1×10^{-5} M), 298 K. [b] Triplet-state lifetime under N_2. [c] Upconverted luminance lifetime, called delayed fluorescence. [d] Quenching constant. [e] Bimolecular quenching constant. [f] TTA-UC quantum yield under N_2, with BODIPY as a standard (Φ_f = 71.2% in CH_3CN).[29] [g] Singlet oxygen quenching quantum yield with $Ru(bpy)_3[2PF_6]$ as a standard (Φ_Δ = 57.1% in CH_3CN),[30] at 298 K.

The singlet oxygen quenching quantum yield of each complex was also measured (Figure 4d). Compared to the mononuclear complexes, the carbazole-bridged dinuclear complexes, **RuCRu** and **IrCIr**, showed considerably higher and desirable singlet oxygen quenching quantum yields (Φ_Δ = 83.3% for **RuCRu**; Φ_Δ = 67.2% for **IrCIr**).

In conclusion, N-substituted carbazole complexes of the d^6 transition metals, Ru(II) and Ir(III), were synthesised. The dinuclear complexes, in which a carbazole moiety is used to generate a conjugated bridging ligand, showed enhanced absorption in the visible region. The attached carbazole moiety gave rise to the mixed ^{3}MLCT and ^{3}ILCT character of the excited states in these complexes. As postulated, the combined effects of two metal centres resulted in significantly improved singlet oxygen quenching quantum yields, when compared to the mononuclear analogues. Although measurements on bimetallic complexes such as these are rare they are showing some consistent messages. They are giving some conclusive insight into the potential improvements possible through the use of multinuclear d^6 complexes towards the practical industrial applications of triplet photosensitisers for TTA-UC technologies and operations.

We thank Drs J. O'Brien, M. Reuther, M. Feeney and G. Hessman for spectroscopic and technical assistance. We thank Prof. J. Zhao for generously facilitating the spectroscopic measurements in Dalian University of Technology. This material is based upon works supported by the Science Foundation Ireland under Research Grant No. SFI/15/TIDA/2952, SFI/15/1A/3046 and SFI/IACA/3413. Y.L. and R.C-K. acknowledge PG studentships from the School of Chemistry, and J.W. from the Irish Research Council. There are no conflicts of interest to declare.

Notes and references

1. S. Campagna, F. Puntoriero, F. Nastasi, G. Bergamini and V. Balzani, in *Photochemistry and Photophysics of Coordination Compounds I*, Springer Berlin Heidelberg, 2007, vol. 280, **ch. 133**, pp. 117-214.
2. Y. J. Yuan, J. Y. Zhang, Z. T. Yu, J. Y. Feng, W. J. Luo, J. H. Ye and Z. G. Zou, *Inorg. Chem.* , 2012, **51**, 4123-4133.
3. Q. Zhao, C. Huang and F. Li, *Chem. Soc. Rev.*, 2011, **40**, 2508-2524.
4. Y. Lu, R. Conway-Kenny, B. Twamley, N. McGoldrick, J. Zhao, S. M. Draper, *ChemPhotoChem.,* 2017, **1**, 544-552.
5. T. N. Singh-Rachford and F. N. Castellano, *Coord. Chem. Rev.* , 2010, **254**, 2560-2573.
6. C. Fan, W. Wu, J. J. Chruma, J. Zhao and C. Yang, *J. Am. Chem. Soc.* , 2016, **138**, 15405-15412.
7. Y. Lu, J. Wang, N. McGoldrick, X. Cui, J. Zhao, C. Caverly, B. Twamley, G. M. Ó Máille, B. Irwin, R. Conway-Kenny and S. M. Draper, *Angew. Chem. Int. ed.* , 2016, **128**, 14908-14912.
8. Y. Lu, N. McGoldrick, F. Murphy, B. Twamley, X. Cui, C. Delaney, G. M. Ó. Máille, J. Wang, J. Zhao and S. M. Draper, *Chem. Eur. J.* , 2016, **22**, 11349-11356.
9. T. F. Schulze and T. W. Schmidt, *Energ. Environ. Sci.* , 2015, **8**, 103-125.
10. Z. Mahmood, A. Toffoletti, J. Zhao and A. Barbon, *J. Lumin.* , 2017, **183**, 507-512.
11. J. Zhao, W. Wu, J. Sun and S. Guo, *Chem. Soc. Rev.,* 2013, **42**, 5323-5351.
12. A. El-ghayoury, A. Harriman, A. Khatyr and R. Ziessel, *J. Phys. Chem. A*, 2000, **104**, 1512-1523.
13. A. Harriman, A. Khatyr and R. Ziessel, *Dalton Trans.*, 2003, **0**, 2061-2068.
14. A. Harriman and R. Ziessel, in *Carbon-Rich Compounds*, Wiley-VCH Verlag GmbH & Co. KGaA, 2006, **ch2**, pp.26-89.
15. A. Harriman, A. Mayeux, C. Stroh and R. Ziessel, *Dalton Trans.* , 2005, **0**, 2925-2932.
16. X. Cui, J. Zhao, Z. Mohmood and C. Zhang, *Chem. Rec.* , 2016, **16**, 173-188.
17. W. Wu, J. Zhao, J. Sun, L. Huang and X. Yi, *J. Mater. Chem. C*, 2013, **1**, 705-716.
18. S. Goswami, R. W. Winkel, E. Alarousu, I. Ghiviriga, O. F. Mohammed and K. S. Schanze, *J. Phys. Chem. A*, 2014, **118**, 11735-11743.
19. W. Wu, J. Zhao, H. Guo, J. Sun, S. Ji and Z. Wang, *Chem. Eur. J.* , 2012, **18**, 1961-1968.
20. J. Wang, Y. Lu, N. McGoldrick, C. Zhang, W. Yang, J. Zhao and S. M. Draper, *J. Mater. Chem. C*, 2016, **4**, 6131-6139.
21. S. Q. Fan, C. Kim, B. Fang, K. X. Liao, G. J. Yang, C. J. Li, J. J. Kim and J. Ko, *J. Phys. Chem. C*, 2011, **115**, 7747-7754.
22. W. Wu, J. Sun, X. Cui and J. Zhao, *J. Mater. Chem. C*, 2013, **1**, 4577-4589.
23. H.-J. Nie, W.-W. Yang, R.-H. Zheng, Q. Shi, H. Chen, J. Yao and Y.-W. Zhong, *Inorg. Chem.* , 2015, **54**, 1272-1282.
24. S. R. Salpage, A. Paul, B. Som, T. Banerjee, K. Hanson, M. D. Smith, A. K. Vannucci and L. S. Shimizu, *Dalton Trans.* , 2016, **45**, 9601-9607.
25. M. Zhou and J. Roovers, *Macromolecules*, 2001, **34**, 244-252.
26. J. B. Flanagan, S. Margel, A. J. Bard and F. C. Anson, *J. Am. Chem. Soc.*, 1978, **100**, 4248-4253.
27. T. Yu, Y. Zeng, J. Chen, Y.-Y. Li, G. Yang and Y. Li, *Angew. Chem. Int. Ed.* , 2013, **52**, 5631-5635.
28. J. Sun, F. Zhong, X. Yi and J. Zhao, *Inorg. Chem.*, 2013, **52**, 6299-6310.
29. W. Wu, H. Guo, W. Wu, S. Ji and J. Zhao, *J. Organ. Chem.* , 2011, **76**, 7056-7064.
30. L. Huang, J. Zhao, S. Guo, C. Zhang and J. Ma, *J. Organ. Chem.* , 2013, **78**, 5627-5637.

View Article Online
DOI: 10.1039/C7CC08535D

This article details the improvements in the photosensitising ability of bimetallic N-carbazole complexes when compared to their mononuclear counterparts.